1   **Functional interactions between post-translationally modified amino acids of**

2   **methyl-coenzyme M reductase in *Methanosarcina acetivorans***

3   Author list – Dipti D Nayak[1, 2, #], Andi Liu[2], Neha Agrawal[3], Roy Rodriguez-Carerro[2],

4   Shi-Hui-Dong[3], Doug A Mitchell[1, 2,4], Satish K Nair[3,5], William W Metcalf[1, 2, *]

5

6   [1]Carl R. Woese Institute of Genomic Biology, University of Illinois, Urbana, USA;

7   [2]Department of Microbiology, University of Illinois, Urbana, USA; [3]Department of

8   Biochemistry, University of Illinois, Urbana, USA; [4]Department of Chemistry,

9   University of Illinois, Urbana, USA; [5]Center for Biophysics & Quantitative Biology,

10   University of Illinois, Urbana, USA

11   **Keywords: Archaea, Methanogens, Post-translational modifications, Methyl-**

12   **coenzyme M reductase**

13

14   [*]Correspondence and requests for materials should be addressed to:

15   William W. Metcalf (metcalf@illinois.edu)

16   Tel: 217-244-1943   Fax: 217-333-0508

17   # Present Address: Department of Molecular and Cell Biology, University of California,

18   Berkeley, CA, USA.

19 **Abstract**

20 Methyl-coenzyme M reductase (MCR) plays an important role in mediating

21 global levels of methane by catalyzing a reversible reaction that leads to the production or

22 consumption of this potent greenhouse gas in methanogenic and methanotrophic archaea.

23 In methanogenic archaea, the alpha subunit of MCR (McrA) typically contains four to six

24 post-translationally modified amino acids near the active site. Recent studies have

25 identified genes that install two of these modifications (thioglycine and 5-(S)-

26 methylarginine), yet little is known about the installation and function of the remaining

27 post-translationally modified residues. Here, we provide *in vivo* evidence that a dedicated

28 SAM-dependent methyltransferase encoded by a gene we designated *mcmA* is

29 responsible for formation of *S*-methylcysteine in *Methanosarcina acetivorans* McrA.

30 Phenotypic analysis of mutants incapable of cysteine methylation suggests that the *S*-

31 methylcysteine residue plays an important role in adaptation to a mesophilic lifestyle. To

32 examine the interactions between the *S*-methylcysteine residue and the previously

33 characterized thioglycine, 5-(S)-methylarginine modifications, we generated *M.*

34 *acetivorans* mutants lacking the three known modification genes in all possible

35 combinations. Phenotypic analyses revealed complex, physiologically relevant

36 interactions between the modified residues, which alter the thermal stability of MCR in a

37 combinatorial fashion that is not readily predictable from the phenotypes of single

38 mutants. Surprisingly, high-resolution crystal structures of the various unmodified MCRs

39 were indistinguishable from the fully modified enzyme, suggesting that interactions

40 between the post-translationally modified residues do not exert a major influence on the

41   physical structure of the enzyme, but rather serve to fine-tune the activity and efficiency

42   of MCR.

Introduction

43

44   Methyl-coenzyme M reductase (MCR) is an unusual and important enzyme,

45   which to date has only been observed in strictly anaerobic, methane-metabolizing archaea

46   (1, 2). In these organisms, MCR catalyzes the reversible inter conversion of methyl-

47   coenzyme M (CoM, 2-methylmercaptoethanesulfonate) and coenzyme B (CoB, 7-

48   thioheptanoylthreoninephosphate) to methane and a coenzyme B-CoM heterodisulfide:

$$CH_3 - S - CoM\ +\ HS - CoB\ \rightleftarrows CH_4\ +\ CoM - S - S - CoB$$
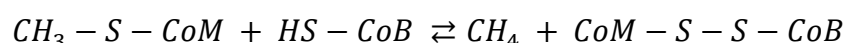
49   Although the methane-oxidizing activity of MCR in **an**aerobic **me**thane-oxidizing

50   archaea (also referred to as ANME) leads to the consumption of *ca.* 90% of the methane

51   produced in marine sediments (3, 4), the methanogenic activity of MCR dominates,

52   leading to the net production of *ca.* 1 gigaton of methane annually (5). Accordingly,

53   methanogenic archaea account for *ca.* 2/3rds of global methane emissions, with

54   significant climate ramifications due to the fact that this abundant greenhouse gas has a

55   warming potential 25 times higher than CO_2 (5–7).

56   Although originally believed to be limited to a few taxa within the Euryarchaoeta

57   (8), recent studies have broadened the diversity of MCR-encoding organisms to

58   encompass all major phyla within the Archaea, including the Asgardarchaeaota, the

59   closest known relatives to eukaryotes (9–12). MCR homologs in some of these

60   uncultivated organisms are thought to be involved in the anaerobic catabolism of short-

61   chain alkanes (1, 11, 13, 14). Thus, canonical MCRs lie within a larger family of 'alkyl-

62   coenzyme M reductases' or ACRs (1, 11). Members of the larger ACR family play

63   pivotal roles in archaeal evolution, climate change and the carbon cycle. They also offer

64   new opportunities for the development of bio-based solutions for the production of

65   methane and other renewable fuels (15). Unfortunately, challenges associated with the

66   cultivation of strictly anaerobic methanogenic archaea, as well as with the *in vitro*

67   activation of MCR have hampered functional characterization of this enzyme (1, 16).

68   Thus, many fundamental properties of this important enzyme remain poorly understood.

69   MCR has a number of unusual traits (17-19). Crystallographic studies of MCR

70   from methane-metabolizing archaea show a $\alpha_2\beta_2\gamma_2$ conformation for the protein complex

71   (Figure 1A) (17–18). The complex possesses two active site pockets, each containing

72   residues from both α-subunits. The active sites also contain tightly bound factor 430

73   (F_{430}), a unique nickel porphinoid cofactor (20, 21) that, to date, has only been observed

74   within MCR. The Ni(I) form of F_{430} is essential for catalysis; however the low reduction

75   potential of the Ni(I)/Ni(II) couple (*ca.* -650 mV) renders F_{430} especially sensitive to

76   oxidative inactivation, which, in turn, has substantially impeded *in vitro* biochemical

77   characterization of MCR (16). The development of new experimental methods has

78   allowed isolation of the fully active Ni(I) form of the enzyme, an especially challenging

79   problem that required nearly twenty years to solve (1, 22). Recent studies of the fully

80   active enzyme suggest that the reaction mechanism involves highly unusual methyl

81   radical and Ni (II)-thiolate intermediate (23). Equally surprising was the discovery of

82   between four to six rare post-translationally modified amino acids within the active site

83   pocket, which eluded detection until high-resolution structures were obtained (18, 19,

84   24). These modified residues have been proposed to play roles in substrate binding,

85   catalysis, or assembly of the MCR complex (24).

86   Mass spectrometric surveys of MCR from diverse methanogenic and

87   methanotrophic archaea show that the modified residues in McrA fall into two broad

5

88   classes: core and variable (24, 25). The core modified amino acids are widely conserved

89   and include N^1-methylhistidine (or 3-methylhistidine), 5-(S)-methylarginine, and

90   thioglycine (Figure 1B). The widespread conservation of these core modifications is

91   exemplified in the recently discovered genes responsible for installation of the

92   thioglycine and 5-(S)-methylarginine modifications, which were originally designated as

93   methanogenesis marker genes because of their universal occurrence in the genomes of

94   sequenced methanogens (26–29). Given that 5-(S)-methylarginine and thioglycine are

95   extremely rare in Nature, yet universally conserved in MCR, it was speculated that these

96   residues must be essential for catalysis (24). Surprisingly, neither the *ycaO-tfuA* locus

97   (MA0165/MA0164), responsible for installing thioglycine, nor the gene (MA4551)

98   encoding the radical SAM methyltransferase responsible for installing 5-(S)-

99   methylarginine is essential for methanogenic growth of *Methanosarcina acetivorans* (26,

100   27). Nevertheless, mutants lacking these genes display severe growth defect on substrates

101   with low free energy yields (such as dimethyl sulfide or acetate) or when the cells are

102   grown under stressful conditions (such as elevated temperatures or oxidative stress) (26,

103   27). Thus, the modifications are important for normal function of MCR and possibly

104   required for methanogens to adapt to non-ideal environments. The gene(s) installing N^1-

105   methylhistidine have yet to be identified; therefore, the biochemical and physiological

106   ramifications of this rare amino acid remain unexplored.

107   The variable modified amino acids include *S*-methylcysteine, 2-(S)-

108   methylglutamine, and 6-hydroxytryptophan (24, 30–32). The phylogenetic distribution of

109   these modifications is uneven, sometimes differing even between closely related strains.

110   For instance, the didehydroaspartate modification is present in the McrA subunit from

111 *Methanothermobacter marburgensis,* but absent in *Methanothermobacter wolfeii* (30).

112 The factors underlying the phylogenetic distribution of variable modified amino acids are

113 currently unknown; however, the non-overlapping occurrence of certain residues, such as

114 *S*-methylcysteine and 6-hydroxytryptophan, suggests that they might be functionally

115 analogous (31).

116 While previous studies have shown the importance of the core modified residues,

117 the function of variable modifications has yet to be addressed. Similarly, the potential

118 interactions between modified residues, as well as their combinatorial influence on MCR

119 structure, stability and activity remain uncharacterized. Here, we identify the gene

120 involved in the installation of *S*-methylcysteine, characterize the physiology of an *M.*

121 *acetivorans* mutant incapable of this modification and assess the thermostability of MCR

122 derived from this strain. We also report the generation and characterization of mutants

123 lacking thioglycine, 5-(S)-methylarginine, and *S*-methylcysteine in all possible

124 combinations, along with the high-resolution crystal structures of all eight MCR variants.

125 Taken together, the data provide evidence of epistastic interactions between modified

126 amino acids in MCR that impact the stability and function of this unusual and important

127 enzyme.

128 **Results**

129 **Crystal Structure of the wild-type MCR from *M. acetivorans***

130 We previously described the addition of an affinity tag that allowed for the facile

131 purification of MCR from *M. acetivorans* cells (33). Aerobic purification and

132 crystallization of the tagged protein from *M. acetivorans* (*Ma*MCR) allowed

133 determination of the structure to a Bragg limit of 1.65 Å using phases calculated by

134   molecular replacement. Relevant data reduction and refinement statistics are provided in

135   Supplemental Table S1.

136   As expected from the high level of sequence conservation (90% identity), the

137   three-dimensional structure of *Ma*MCR displays an architecture that is nearly identical to

138   that of MCR from *Methanosarcina barkeri* (*Mb*MCR; PDB code: 1E6Y), with a root

139   mean square (RMS) deviation of all Cα atoms of 0.24 Å. The protein complex

140   crystallized as a $\alpha_2\beta_2\gamma_2$ assembly with one complex in the crystallographic asymmetric

141   unit. Electron density for the affinity tag was not evident (Figure 1A). Notably, the active

142   site of *Ma*MCR shows electron density features corresponding to the F_{430} cofactor, as

143   well as for the coenzyme M and coenzyme B, showing that the affinity tag does not

144   disrupt the association of these cofactors. Given the 1.65 Å resolution of the structure,

145   clear electron density features indicative of modified amino acids are evident for the

146   following residues of α subunit: *N*-methylation at His271, 5-(S)-methylation of Arg285,

147   *S*-methylation of Cys472, and the presence of a thioamide bond at Gly465 (Figure 1B).

148   Desaturation of the Cα-Cβ linkage at Asp470 to yield a didehydroasparate cannot be

149   discerned at this resolution, but was confirmed by mass-spectrometry (see below).

150   Therefore, we have included the didehydroasparate modification in the structural model.

151   **Identification of a methyltransferase mediating the *S*-methylcysteine modification of**

152   **Cys472 in McrA from *M. acetivorans***

153   Based on its proximity to the structural genes encoding MCR in *M. acetivorans,* we

154   hypothesized that a SAM-dependent methyltransferase belonging to the InterPro

155   superfamily IPR29063 (MA4545; AAM07884.1; Q8THH2) would be involved in the

156   post-translational methylation of one or more amino acids in McrA (Figure 2A) (24, 32).

8

157   Significantly, phylogenetic profiling of the MA4545 locus revealed that homologs are

158   absent in two hyperthermophilic methanogens (*Methanocaldococcus janaschiii* and

159   *Methanopyrus kandleri*) that have been shown to lack *S*-methylcysteine within MCR

160   (24). The phylogenetic tree of MA4545 is incongruent with both the MCR phylogeny and

161   the reference phylogeny of archaea built with concatenated housekeeping genes (Figure

162   2B) (9, 11). Accordingly, it seems likely that a gene loss event and subsequent HGT

163   event in the last common ancestor of the *Methanosarcinaceae* family is responsible for

164   the shared ancestry of this locus between members of the *Methanosarcina* genus and the

165   distantly related *Methanobacteriales* (Figure 2B).

166   To test the hypothesis that MA4545 is responsible for *S*-methylation of Cys472 in

167   McrA, we deleted the gene in *M. acetivorans* using recently developed Cas9-based

168   genome editing tools (34). Matrix-assisted laser desorption/ionization time-of-flight mass

169   spectrometry (MALDI-TOF-MS) showed that the McrA tryptic peptide containing the

170   Cys residue of interest was 14 Da lighter in the mutant than in the corresponding peptide

171   from wild-type, consistent with loss of a methyl group in the mutant (Figure 3C). The

172   peptide was then subjected to high-resolution and tandem mass spectrometry, which

173   confirmed the lack of Cys472 methylation in the mutant (Supplementary Figure S1).

174   Taken together, these data clearly indicate that the MA4545 locus is involved in *S*-

175   methylation of the Cys472 residue in McrA from *M. acetivorans.* Accordingly, we

176   propose renaming this gene *mcmA* (**m**ethyl**c**ysteine **m**odification). Mass analysis of

177   tryptic peptides containing the remaining modified amino acids showed that all were

178   maintained in the *mcmA* mutant (Figure 3 and Supplementary Figure S2). Thus,

179   installation of these modifications does not require the presence of methylcysteine.

180   The Δ*mcmA* mutant was viable on all growth substrates tested (Figure 4A).

181   Relative to wild-type, the mutant grew 30% slower on dimethyl sulfide (DMS) (p = 0.002

182   for an unpaired t-test with the means of three biological replicates) (Figure 4A). A 12%

183   decrease in growth yield (measured as the maximum optical density at 600 nm) was

184   observed on trimethylamine (TMA) (p = 0.018) (Figure 4B). Thus, even though the *S*-

185   methylation of Cys472 in McrA is dispensable in *M. acetivorans*, it is clearly important

186   for methanogenic growth on certain substrates. Curiously, the Δ*mcmA* mutant had better

187   growth rates and yields than the wild type on some substrates, with more pronounced

188   improvements at higher temperatures (Figure 4).

189   **Generation of combinatorial mutants of *M. acetivorans* lacking the thioglycine, 5-**

190   **(S)-methylarginine, and *S*-methylcysteine modification in McrA**

191   Since the α subunit of MCR contains multiple modified amino acids in spatial

192   proximity (Figure 1B), epistasis between these residues may be important for optimal

193   enzyme function. To test this, we generated deletion mutants lacking the genes

194   responsible for installing *S*-methylcysteine, thioglycine and 5-(S)-methylarginine in all

195   possible combinations (Supplementary Figure S3A). These include MA4551, which we

196   have renamed *mamA* (**m**ethyl**a**rginine **m**odification) to better reflect its function

197   (Supplementary Figure S4 and (27, 28)) and *ycaO-tfuA* (MA0165/MA0164), which

198   coverts glycine to thioglycine (26, 29). The phenotypic analyses described below were

199   carried out in mutants that encode wild-type MCR, while biochemical and structural

200   studies were conducted with MCR purified from a second set of mutants that encode a

201   modified *mcrG* allele (encoding the γ subunit of MCR) with an N-terminal a tandem-

10

202   affinity purification tag comprising of a twin-Strep tag and a 3×FLAG tag (hereafter

203   referred to as TAP tag) (Supplementary Figure S3B).

204   Modified McrA residues from *M. acetivorans* are independently installed

205   Although the loss of single post-translational modifications does not effect the

206   installation of other modifications (26, 27), the behavior of mutants lacking a

207   combination of modified residues was unknown. To examine this, we identified all

208   known post-tanslatioanlly modified amino acids in McrA from each of the mutants by

209   MALDI-TOF-MS of peptides produced upon digestion with trypsin or a combination of

210   the endoproteinases AspN and GluC (Figure 3). Additionally, high-resolution and tandem

211   mass spectrometry techniques were employed to confirm the identity and location of each

212   modification on the corresponding peptides (Supplementary Figures S5-S8). The

213   modification state of McrA from *M. acetivorans* perfectly corresponds to the genotype of

214   the mutant from which the protein was purified (Figure 3). These data validate the

215   expected modification state of the mutants, while showing that the 5-(S)-methylarginine,

216   thioglycine, and *S*-methylcysteine are independently installed.

217   Growth analyses of combinatorial mutants reveal complex interactions between

218   modified amino acids in McrA

219   Although direct interactions between the modified residues McrA are not apparent in

220   the crystal structure, indirect interactions have been suggested to be important for enzyme

221   catalysis (18, 19). For instance, both the thioglycine and *S*-methylcysteine are within van

222   der Waals contact of Leu468, and such contacts are thought to cooperatively influence

223   the local structure near the active site (Figure 1). To test whether these indirect

224   interactions are physiologically relevant, and to uncover the nature of these interactions,

11

225   we examined the growth phenotypes of mutants lacking the three modified residues in all

226   possible combinations.

227   Growth analyses were performed on four different substrates: methanol (125 mM),

228   TMA (50 mM), DMS (20 mM), and acetate (40 mM), which require substantially

229   different methanogenic pathways and a wide range of free energy yields ($\Delta G°'$/mol CH_4)

230   (Supplementary Figure 9). Apart from the inability of the $\Delta ycaO$-$tfuA$/$\Delta mcmA$ double

231   mutant to grow on DMS, all other mutants were viable on all the substrates tested (Figure

232   4A; Supplementary Tables S2-S13).   Indeed, the $\Delta ycaO$-$tfuA$/$\Delta mcmA$ mutant had the

233   most severe growth defect on all substrates tested, corroborating the hypothesis that the

234   thioglycine and S-methylcysteine modifications interact synergistically (Figure 4A).

235   Surprisingly, the triple deletion mutant grew faster than the $\Delta ycaO$-$tfuA$/$\Delta mcmA$ mutant,

236   indicating that the unmodified Arg285 residue alleviates the growth defect observed in

237   the absence of both the thioglycine and S-methylcysteine modifications (Figure 4A and

238   4B). On substrates with high free energy yields (methanol and TMA), most of the

239   mutants lacking one or more of the modified residues grew as well as, or better than, the

240   wild-type strain (Figure 4A). However, substantial growth rate defects, of varying

241   magnitude depending on the strain, were observed on substrates with low free energy

242   yields (DMS and acetate) (Figure 4A).

243   In a previous study, we observed that the $\Delta ycaO$-$tfuA$ mutant has a severe growth

244   defect at elevated temperatures, which suggested that the thioglycine modification plays

245   in a role in stabilizing the active site of MCR (26). Therefore, we assayed the growth

246   phenotype of all mutants on 50 mM TMA at 29 °C, 36 °C, and 42 °C, where 36 °C

247   represents the optimal growth temperature. While all mutants grew at every temperature,

12

248   the growth phenotypes varied dramatically (Figure 4C, Figure 4D, Supplementary Tables

249   S9-S13). Indeed, the mutant lacking all three modified residues grew 18% faster than

250   wild-type at 29 °C (p = 0.001) (Figure 4C, Figure 4D, Supplementary Table 10).

251   Significantly, the mutant lacking only the *S*-methylcysteine modification had a 20%

252   increase in growth rate relative to wild-type at 42 °C (p = 0.018) (Figure 4C,

253   Supplementary Table 11), indicating that this modification might be involved in the

254   adaptation of MCR to growth under mesophilic conditions. In aggregate, the growth

255   phenotypes of the double or triple mutants could not have been predicted by the studying

256   the single mutants in isolation, which is a strong indicator of extensive, physiologically

257   relevant, interactions between modified McrA amino acids.

258   **Interactions between thioglycine and 5-(S)-methylarginine are important for the in**

259   **vitro thermal stability of MCR**

260   The sign and magnitude of interactions between modified amino acids was

261   especially evident during growth at elevated temperatures (Figure 4C and Figure 4D). To

262   delve deeper into this phenotype, we investigated the global stability of the purified MCR

263   complex using a SYPRO Orange-based thermofluor assay (35). Consistent with prior

264   work (27), the melting temperature (T_m) of MCR from the $\Delta mamA$ mutant was

265   significantly lower (-6.5 °C; p< 0.001) than wild-type, whereas the T_m of the MCR from

266   the $\Delta mcmA$ mutant was indistinguishable from wild-type (Figure 5A). Notably, the

267   presence of Gly465 (as opposed to thioglycine) restored the T_m of MCR with an

268   unmodified Arg285 residue, irrespective of whether Cys472 was modified (Figures 5B

269   and 5C). Taken together, these data suggest that the 5-S-methylarginine and thioglycine

270   modifications, as well as interactions between them, influence the thermal stability of

13

271 MCR, again in ways that are not easily predicted from the stability of MCR lacking

272 single modifications.

Structural analyses of combinatorial mutants

274   To gain molecular insights into the nature of the *S*-methylcysteine, thioglycine

275 and 5-(S)-methylarginine interactions and their influence on the activity and stability of

276 MCR, we solved the crystal structure of TAP-tagged MCR derived from each of the

277 aforementioned mutants at resolutions between 1.9-2.3 Å (Supplementary Table 1).

278 Crystals of the different variants occupy different unit cell settings, which rules out

279 crystal packing artifacts as a potential source of bias between the structures. Examination

280 of unbiased electron density maps reveals the presence and/or absence of the expected

281 modified residues in the MCR variants obtained from the eight mutants.

282   The global structures of MCR variants purified from the combinatorial mutants

283 remain unchanged relative to the wild-type, consistent with the lack of long-range

284 interactions between the modified residues. Surprisingly, the structural analyses show

285 that there are also no significant local changes to the active site pocket in any of the

286 variants (Figure 6). Given the observation that the thioglycine and 5-(S)-methylarginine

287 modifications influence thermal stability, we had expected the corresponding structures

288 to reveal active site perturbations that would cause these differences. The similarity of the

289 structures is also surprising given the extensive side chain interactions that occur at the

290 site of each particular modification, which span the different subunits of MCR. We note,

291 however, that because the crystal structures are likely to capture the lowest energy

292 conformational state of each of the variant, dynamic movements that may occur at the

14

293   voids created by removal of the amino acid modifications are unlikely to be captured in

294   these static structures.

295   **Discussion**

296   All characterized MCRs contain a set of core and variable modified amino acids

297   near the active site (1, 9, 24). For the last two decades, researchers have speculated on the

298   role of these modifications vis-à-vis the function of MCR. These hypotheses have ranged

299   from certain modified residues being critical for activity to others playing minor roles (1).

300   Recent studies have identified genes installing thioglycine and 5-(*S*)-methylarginine and

301   shown that neither of these residues is essential for catalysis, although they might be

302   important for the structural integrity of the MCR complex (26, 27). Here, we build on our

303   previous study (26) by identifying a SAM-dependent methyltransferase involved in the

304   installation of *S*-methylcysteine, a variable modified amino acid, and also uncovering

305   evidence that epistasis between the three modified residues is also important for MCR *in*

306   *vivo.*

307   The data presented above show that a dedicated SAM-dependent

308   methyltransferase (renamed *mcmA*) is responsible for the *S*-methylation of a conserved

309   Cys472 residue in McrA derived from *M. acetivorans* (Figure 3). Consistent with this

310   conclusion, the C-terminus of McmA contains conserved residues that are involved in

311   binding SAM. Thus, we suspect that the N-terminal domain of the protein, which lacks

312   any identifiable domains, is involved in substrate recognition and/or binding. Homologs

313   of McmA are especially widespread in methanogens that grow at moderate temperatures;

314   however, they are absent from hyperthermophilic methanogens like *M. kandleri* and *M.*

315   *janaschii,* as well as from psychrophilic methanogens like *Methanococcoides burtonii* or

15

316   *Methanogenium frigidum* (Figure 2B). This phylogenetic distribution suggests that the *S*-

317   methylcysteine modification is involved in the adaptation of MCR to mesophilic

318   environments (Figure 2B). This idea is supported by our observation that the Δ*mcmA*

319   mutant grew faster than the parent strain at both elevated (42 °C) and reduced (29 °C)

320   temperatures (Figure 4C). Despite enhanced growth at high temperatures, the thermal

321   stability of the MCR complex lacking the *S*-methylcysteine modification is

322   indistinguishable from wild-type (Figure 5A). This indicates that the presence of *S*-

323   methylcysteine does not improve the global stability of the enzyme complex.

324   Furthermore, the structure of MCR from this mutant is essentially identical to that of the

325   wild-type, including within the active site pocket near the modification site (Figure 6).

326   Thus, we suspect that the temperature-dependent phenotypes of strains lacking *S*-

327   methylcysteine are related to catalysis rather than structure. Curiously, homologs of

328   McmA are absent in a few mesophilic methanogens, like the gut-associated

329   *Methanomassiliicoccus* species (Figure 2B). Whether the *S*-methylcysteine modification

330   is indeed absent in this organism, or whether another protein is capable of installing this

331   modification, remains to be determined.

332   Despite the fact that the modified residues in MCR are in spatial proximity, only

333   independent functions have been proposed for these unusual amino acids (*i.e.* they do not

334   exert any influence on each other (22, 24). Our *in vivo* growth data, as well as the *in vitro*

335   MCR thermal stability data, clearly show that each of the characterized modifications

336   influences the function of the others. Moreover, our data demonstrate that the function of

337   these modified amino acids is not reflected in static crystal structures. Thus, it seems

338   highly likely that they exert their effects during enzyme turnover. Whether these effects

16

339   are related to substrate binding and catalysis, or conformational/allosteric communication

340   between the two active sites, as in the proposed two-stroke catalytic mechanism (1, 36),

341   will await the *in vitro* characterization of active MCR from our mutants. Unfortunately,

342   given its sensitivity to oxidative inactivation, *in vitro* kinetic characterization of MCR is

343   especially problematic. The most widely used activation protocol relies hydrogenase

344   activity (16). Unfortunately, as *M. acetivorans* does not produce active hydrogenases, this

345   activation procedure is not directly transferable to our system. An alternate protocol

346   involving pretreatment of cells with sodium sulfide to generate the Ni(III) from of the

347   enzyme, followed by reduction of the purified enzyme with the strong reductant titanium

348   citrate (37), has not been successful in our hands. Thus, kinetic characterization of the

349   various unmodified MCR derivatives reported here currently remains out of reach.

350   Until a method for activation of *M. acetivorans* MCR is achieved, hypotheses for

351   the functional roles of the modified MCR residues must rely on physiological data. MCR

352   comprises *ca.* 10% of the total cellular protein and is often considered to be the rate-

353   limiting step during methanogenic growth (23, 38). Therefore, if the loss of modifications

354   alters MCR activity or the binding affinity for substrates, one would expect to see

355   changes in growth rates and yields. For this reason, we assayed growth rates and yields

356   on a variety of substrates that are used by distinct methanogenic pathways

357   (Supplementary Figure 9). We note that a recent review suggested that anabolism is the

358   rate-limiting step of methanogenic growth in batch cultures (1). While this is may be

359   possible, it is difficult to rationalize this idea with the observation of faster (and slower)

360   growth in the mutants described here, because MCR modification state is the only

361   variable in these experiments and because MCR is not known to be involved in

17

362   anabolism. Consistent with the idea that MCR is rate-limiting, we observed numerous,

363   significant growth phenotypes. These include examples where the mutants performed

364   significantly worse or significantly better than strains with fully modified MCR. The

365   improved growth of modification-deficient mutants is especially surprising given the

366   extensive conservation of post-translationally modified residues in MCR. Indeed, the

367   triple mutant lacking thioglycine, *S*-methylcysteine and 5-(*S)*-methylarginine grew better

368   than the parental strain under nearly every condition tested, which begs the question of

369   why MCR is modified at all. A satisfactory answer to this question remains elusive.

370   The interactions between the modified residues are complex and difficult to

371   predict from the phenotypes of double and single mutants; nevertheless, the observed

372   phenotypes hint at possible mechanisms. The thioglycine and *S*-methylcysteine residues

373   both interact with Leu468; whereas Leu468 and thioglycine also interact with Asn501, an

374   important residue involved in coenzyme B binding (Figure 1B). Therefore, one

375   hypothesis is that thioglycine and *S*-methylcysteine together facilitate the interaction

376   between the thiol group of coenzyme B and the side-chain nitrogen of Asn501 to

377   influence the K_m for coenzyme B. Likewise, the *S*-methylcysteine is in close proximity to

378   His382 from McrB at the intersubunit interface and might similarly affect the binding of

379   coenzyme B. This hypothesis is supported by the observation that the most severe growth

380   defects are seen in mutants lacking *S*-methylcysteine and thioglycine. Curiously, our

381   growth data also reveal that, despite being >14 Å away from Gly465 or Cys472, the

382   unmodified Arg285 mitigates the deleterious effects of these unmodified amino acids

383   (Figure 4). As each of the modified residues are involved in contacts within and across

384   different subunits of MCR, we speculate that removal of the modifications has minimal

18

385   effects on the structure. Essentially, deletion of the post-translational modification creates

386   voids in the central core of MCR, adjacent to the active site, which compromises the

387   catalytic stability of the enzyme during catalysis without changing the lowest entropy

388   conformational state that is captured by X-ray crystallography.

389   Epistasis between modified residues was also evident when we characterized the

390   global stability of the MCR complex *in vitro.* Among the three modified amino acids

391   only 5-(*S*)-methylarginine plays a significant role in mediating the thermal stability of

392   MCR (Figure 5A). Neither thioglycine nor *S*-methylcysteine influence thermal stability in

393   isolation, but the unmodified Gly465 residue compensates for the deleterious impact of

394   an unmodified Arg285 on global stability. A comparison of the crystal structures of the

395   variant lacking 5-methylation on Arg285, with that lacking both this modification as well

396   the thioglycine failed to reveal any notable changes in the active site that may account for

397   the compensatory effects observed on thermal stability. Hence, it is likely that the effect

398   of the mutations occurs either on the unfolded state of MCR or on transient intermediates

399   formed during the folding process, without affecting the lowest energy ground state

400   observed in the crystal structures.

401   In summary, recent studies have changed our view of the modified amino acids in

402   MCR from biochemical novelties to evolutionary spandrels: features that are an offshoot

403   of adaptation rather than a direct product thereof. Despite this paradigm shift, it is still

404   perplexing as to why members of the ACR family contains between four to six unique

405   and rare post-translational modifications. If the role of these modifications is to fill voids

406   or contort the amino acid backbone, why didn't the twenty standard amino acids suffice?

407   It is entirely feasible that the functions of these modifications extend beyond the scope of

408 conditions that can be tested in a laboratory setting. As we sample diverse groups of

409 methanogenic archaea, ANMEs, and even anaerobic alkane oxidizing archaea and

410 identify the pattern of modifications in their ACRs, maybe the underlying reasons will

411 become apparent. In the near future, we expect that broader surveys of diverse ACRs

412 coupled with laboratory-based genetic experiments will enable the design of appropriate

413 experiments to tease apart the role of these unusual modified amino acids.

414

415 **Materials and Methods**

416   **Phylogenetic analyses.** One hundred closest homologs were extracted from the

417 NCBI non-redundant protein database using the McmA amino acid sequence (MA4545;

418 AAM07884.1; Q8THH2) or the MamA amino acid sequence (MA4551, AAM07890;

419 Q8THG6) as queries in BLAST-P searches. Any partial sequences (i.e. sequences < 300

420 amino acids in length) were discarded and the full-length protein sequences were aligned

421 using the MUSCLE plug-in (39) with default parameters in Geneious version R9 (40).

422 Approximate maximum-likelihood trees were generated using FastTree version 2.1.3

423 SSE3 using the Jones-Taylor-Thornton (JTT) model + CAT approximation with 20 rate

424 categories. Branch support was calculated using the Shimodaira-Hasegawa (SH) test with

425 1,000 resamples. Trees were displayed using Fig Tree v1.4.3

426 (http://tree.bio.ed.ac.uk/software/figtree/).

427   **Construction of gene-editing plasmids.** All mutations in *M. acetivorans* were

428 introduced using a Cas9-based genome editing technique (34). Mutagenic plasmids were

429 derived from pDN201, a base vector containing Cas9 from *Streptococcus pyogenes* under

430 the control of the tetracycline-inducible pMcrB(tetO1) promoter. A double-stranded

431   DNA fragment, synthesized as a gblock (Integrated DNA Technologies, Coralville, IA,

432   USA), expressing one or more single guide (sg) RNAs targeting the locus of interest was

433   introduced at the *AscI* site in pDN201 using the HiFi assembly kit (New England Biolabs,

434   Ipswich, MA, USA). Subsequently, a homology repair template, either generated by PCR

435   amplification or synthesized as a gblock (Integrated DNA Technologies, Coralville, IA,

436   USA), was introduced at the *PmeI* site in the sgRNA-containing vector using the HiFi

437   assembly kit (New England Biolabs, Ipswich, MA, USA). A cointegrate of the resulting

438   plasmid and pAMG40 (containing the pC2A replicon) was generated using the BP

439   clonase II enzyme master mix (Thermo Fisher Scientific, Waltham, MA, USA) to enable

440   autonomous replication of the mutagenic vector in *M. acetivorans*. All primers used to

441   generate and verify plasmids are listed in Supplementary Table S15 and the plasmids

442   used in this study are listed in Supplementary Table S16. Standard techniques were used

443   for the isolation and manipulation of plasmid DNA. All pDN201-derived plasmids were

444   verified by Sanger sequencing at the Roy J. Carver Biotechnology Center, University of

445   Illinois at Urbana-Champaign and all pAMG40 cointegrates were verified by restriction

446   endonuclease analysis.

447   ***In silico* design of sgRNAs for gene editing.** All target sequences used for Cas9-

448   mediated genome editing in this study are listed in Supplementary Table S17. Target

449   sequences were chosen using the CRISPR site finder tool in Geneious version R9. The *M.*

450   *acetivorans* chromosome and the plasmid pC2A were used to score off-target binding

451   sites.

452   ***E. coli* growth and transformations.** WM4489, a DH10B derivative engineered

453   to control copy-number of oriV-based plasmids (41), was used as the host strain for all

454   plasmids generated in this study (Supplementary Table S16). Electrocompetent cells of

455   WM4489 were generated as described in (41) and transformed by electroporation at 1.8

456   kV using an *E. coli* Gene Pulser (Bio-Rad, Hercules, CA). Plasmid copy number was

457   increased dramatically by supplementing the growth medium with sterile rhamnose to a

458   final concentration of 10 mM. The growth medium was supplemented with a sterile stock

459   solution of chloroamphenicol to a final concentration of 10 μg/mL and/or kanamycin to a

460   final concentration of 25 μg/mL as appropriate.

461   **Transformation of *M. acetivorans*.** All *M. acetivorans* strains used in this study

462   are listed in Supplementary Table S18. Liposome-mediated transformation was used for

463   *M. acetivorans* as described previously (42) using 10 mL of late-exponential phase

464   culture of *M. acetivorans* and 2 μg of plasmid DNA for each transformation. Puromycin

465   (CalBiochem, San Diego, CA) was added to a final concentration of 2 μg/mL from a

466   sterile, anaerobic stock solution to select for transformants containing the *pac* (puromycin

467   transacetylase) cassette. The purine analog 8-aza-2,6-diaminopurine (8ADP) (R. I.

468   Chemicals, Orange, CA) was added to a final concentration of 20 μg/mL from a sterile,

469   anaerobic stock solution to select against the *hpt* (phosphoribosyltransferase) cassette

470   encoded on pC2A-based plasmids. Plating on HS medium containing 50 mM TMA

471   solidified with 1.7 % agar was conducted in an anaerobic glove chamber (Coy Laboratory

472   Products, Grass Lake, MI) as described previously (43). Solid media plates were

473   incubated in an intra-chamber anaerobic incubator maintained at 37 °C with $N_2/CO_2/H_2S$

474   (79.9/20/0.1) in the headspace as described previously (43).

475   **Growth assays for *M. acetivorans*.** *M. acetivorans* strains were grown in single-

476   cell morphology (44) in bicarbonate-buffered high salt (HS) liquid medium containing

477 one of the following: 125 mM methanol, 50 mM trimethylamine hydrochloride (TMA),

478 40 mM sodium acetate, or 20 mM dimethylsulfide (DMS). Most substrates were added to

479 the medium prior to sterilization. DMS was added from an anaerobic stock solution

480 maintained at 4 °C immediately prior to inoculation. For growth analyses, 10 mL cultures

481 were grown in sealed Balch tubes with N_2/CO_2 (80/20) at 8-10 psi in the headspace.

482 Growth measurements were conducted with three independent biological replicates

483 derived from colony-purified isolates. Each replicate was acclimated to the growth

484 substrate or growth temperature for a minimum of five generations prior to quantitative

485 growth measurements. A 1:10 dilution of late-exponential phase cultures was used as the

486 inoculum for growth analyses.

487   **Affinity purification of MCR for MS analyses and Thermofluor assays.** TAP-

488 tagged MCR was purified from 250 mL of late-exponential phase culture grown in HS +

489 50 mM TMA at 36 °C. Protein purification was performed under aerobic conditions and

490 cells were harvested by centrifugation (3,000 × g) for 15 min at 4 °C. The cell pellet was

491 lysed in 10 mL salt-free wash buffer (50 mM NaH_2PO_4, pH = 8.0) and sodium chloride

492 was added to a final concentration of 300 mM post-lysis. The cell lysate was treated with

493 DNase and clarified by centrifugation (17,500 × g) for 30 min at 4 °C. The supernatant

494 fraction was loaded on a column containing 1 mL Streptactin Superflow Plus slurry (50%

495 suspension; QIAGEN, Germantown, MD, USA) equilibrated with 8 mL of the wash

496 buffer (50 mM NaH_2PO_4, 300m M NaCl, pH = 8.0). The column was washed four times

497 with 2 mL of Wash buffer and the purified protein was eluted in four fractions with 0.5

498 mL Elution buffer (50 mM NaH_2PO_4, 300 mM NaCl, 50 mM biotin, pH = 8.0) per

499 fraction. The protein concentration in each fraction was estimated using the Coomassie

23

500   Plus (Bradford) assay kit (Pierce Biotechnology, Thermo-Scientific, Rockford, IL, USA)

501   with BSA (bovine serum albumin) as the standard per the manufacturer's instructions.

502   The highest protein concentration (*ca.* 1 mg/mL) was obtained in fraction 2 therefore this

503   fraction was used to conduct the Thermofluor assay. To visualize the purified protein, 10

504   µL of fraction 2 was mixed with an equal volume of 2× Laemmli sample buffer (Bio-

505   Rad, Hercules, CA) containing 5% β-mercaptoethanol, incubated in boiling water for 10

506   min, loaded on a 4-20% gradient Mini-Protean TGX denaturing SDS-PAGE gel (Bio-

507   Rad, Hercules, CA) and run at 70 V until the dye-front reached the bottom of the gel. The

508   gel was stained using the Gel Code Blue stain reagent (Thermo Fisher Scientific,

509   Waltham, MA) as per the manufacturer's instructions.

510   **Proteolytic digestion of purified MCR.** For trypsinolysis, 300 µg of purified

511   MCR was digested with mass spectrometry (MS)-grade trypsin (1:100 *w/w* ratio;

512   Thermo-Scientific, Rockford, IL, USA) at a final MCR concentration of 1 mg/mL in 50

513   mM NH_4HCO_3 at 37 °C for 14 h. The tryptic peptides were desalted using a C-18 zip-tip

514   using aqueous acetonitrile or further purified by high performance liquid chromatography

515   (HPLC) prior to MS analysis. For AspN and GluC double digestion, 50 µg of purified

516   MCR was digested with endoproteinase GluC (1:200 *w/w* ratio; New England BioLabs,

517   Ipswich, MA, USA) and endoproteinase AspN (1:200 *w/w* ratio; Promega, Madison, WI,

518   USA) at a final MCR concentration of 1 mg/mL with the addition of 20% AspN 1×

519   buffer (New England BioLabs, Ipswich, MA, USA) and GluC 2× buffer (New England

520   BioLabs, Ipswich, MA, USA) at 37 °C for 24 h. The resulting digested peptides were

521   desalted with C-18 zip-tips using acetonitrile with 0.1% formic acid prior to MS analysis.

24

522   **HPLC purification of MCR tryptic fragments.** The aforementioned tryptic

523   peptides were subjected to HPLC analysis using a C18 column (Macherey-Nagel, 4.6 ×

524   250 mm, 5 μm particle size). Acetonitrile and 0.1% (*v/v*) formic acid were used as the

525   mobile phase. A linear gradient of 20 to 80% acetonitrile over 23 min at 1 mL/min was

526   used to separate the peptides. Fractions were collected at one-minute intervals and

527   analyzed by matrix-assisted laser desorption/ionization time-of-flight mass spectrometry

528   (MALDI-TOF-MS) with alpha-cyano-4-hydroxycinnamic acid (CHCA) as matrix using a

529   Bruker UltrafleXtreme instrument (Bruker Daltonics, Billerica, MA, USA) in reflector

530   positive mode at the University of Illinois School of Chemical Sciences Mass

531   Spectrometry Laboratory. The fragment of interest elutes between 11-12 min regardless

532   of the modification. The fraction was dried under vacuum using a Speedvac concentrator

533   (Thermo Fisher Scientific, Waltham, MA, USA) for further analysis.

534   **MS analysis of MCR peptidic fragments.** MALDI-TOF-MS analysis was

535   performed on the desalted MCR fragments as described above. For high-resolution

536   electrospray ionization (ESI) MS/MS, samples were dissolved in 35% acetonitrile and

537   0.1% formic acid and directly infused using an Advion TriVersa Nanomate 100 into a

538   ThermoFisher Scientific Orbitrap Fusion ESI-MS. The instrument was calibrated weekly,

539   following the manufacturer's instructions, and tuned daily with Pierce LTQ Velos ESI

540   Positive Ion Calibration Solution (Thermo Fisher Scientific, Waltham, MA). The MS was

541   operated using the following parameters: resolution, 100,000; isolation width (MS/MS), 1

542   *m/z*; normalized collision energy (MS/MS), 50; activation q value (MS/MS), 0.4;

543   activation time (MS/MS), 30 ms. Data analysis was conducted using the Qualbrowser

25

544   application of Xcalibur software (Thermo Fisher Scientific, Waltham, MA, USA).

545   HPLC-grade reagents were used to prepare samples for mass spectrometric analyses.

546   **Thermofluor Assay.** A 5000× concentrate of SYPRO Orange protein gel stain in

547   Dimethylsulfoxide (DMSO) (Thermo Fisher Scientific, Waltham, MA, USA) was diluted

548   with the elution buffer to generate a 200× stock solution. Purified MCR from fraction 2

549   was diluted to *ca.* 500 µg/mL with the elution buffer. 5 µL of the 200× stock solution of

550   SYPRO Orange protein gel stain was added to 45 µL of purified protein with a

551   concentration of *ca.* 500 µg/mL in 96-well optically clear PCR plates. A melt curve was

552   performed on a Mastercycler ep realplex machine (Eppendorf, Hamburg, Germany) using

553   the following protocol: 25 °C for 30 s, ramp to 99 °C over 30 min, return to 25 °C for 30

554   s. SYPRO Orange fluorescence was detected using the VIC emission channel and the

555   temperature corresponding to the inflection point of the first derivative (-dI/dT) was

556   determined to be the melting temperature (T_m). Appropriate no-dye controls and no-

557   protein controls were examined and each sample was run in triplicate. The Thermofluor

558   assay was conducted within 12 h of protein purification.

559   **Affinity purification of MCR from *M. acetivorans* for crystallography.** TAP-

560   tagged MCR was purified as described above for the MS analyses and Thermofluor

561   assays with the following modifications. Protein was purified under aerobic conditions

562   from 500 mL of late-exponential phase culture grown in HS + 50 mM TMA at 36 °C.

563   The crystallography wash buffer comprised of 100 mM Tris.HCl, 300 mM NaCl and 2

564   mM dithiothreiotol (DTT) at pH 8. The crystallography elution buffer contained 2.5 mM

565   desthiobiotin in addition to the other components of the crystallography wash buffer.

566   Four 250μL fractions of purified MCR were collected and visualized using a 12% Mini-

567   Protean TGX denaturing SDS-PAGE gel (Bio-Rad, Hercules, CA).

568   **Crystallization of MCR from *M. acetivorans*.** MCR was concentrated to 25 mg/ml prior

569   to crystallization via ultrafiltration. The crystallization trials utilized 2 μl sitting drops

570   composed of 0.9: 0.9: 0.2 (protein: reservoir solution: additive screen) that were

571   equilibrated against a 500 μl volume of the reservoir solution at room temperature. The

572   reservoir solution contained 0.2 M ammonium acetate, 0.1 M sodium acetate, pH = 4 and

573   15 % (w/v) PEG 4000. Similarly, the MCR variants were concentrated to 3- 30 mg/ml.

574   The crystals were obtained in a hanging drop format composed of 2 μl mixture of 0.9:

575   0.9: 0.2 (protein: reservoir solution: additive screen) equilibrated against the same

576   reservoir solution as the wild-type. Prior to freezing by vitrification in liquid nitrogen,

577   crystals were soaked in reservoir solution supplemented with an additional 20 % (v/v)

578   glycerol or 30 % (w/v) PEG 4000.

579

580   **Acknowledgements.**

27

589   Department of Microbiology at the University of Illinois at Urbana-Champaign. The

590   Bruker UltrafleXtreme MALDI TOF/TOF mass spectrometer was purchased in part with

591   a grant from the National Institutes of Health (S10 RR027109 A).

592

References

594   1.   Thauer RK (2019) Methyl (Alkyl)-Coenzyme M Reductases: Nickel F-430-

595   Containing Enzymes Involved in Anaerobic Methane Formation and in Anaerobic

596   Oxidation of Methane or of Short Chain Alkanes. *Biochemistry*.

597   https://doi.org/10.1021/acs.biochem.9b00164

598   2.   Rosenzweig AC (2016) Methane-Oxidizing Enzymes: An Upstream Problem in

599   Biological Gas-to-Liquid Conversion. *J Am Chem Soc*138(30):9327-9340.

600   3.   Valentine DL, Reeburgh WS (2000) New Perspectives on Anaerobic Methane

601   Oxidation. *Environ Microbiol* 2(5):477–484.

602   4.   Knittel K, Boetius A (2009) Anaerobic Oxidation of Methane: Progress With an

603   Unknown Process. *Annu Rev Microbiol* 63:311–34.

604   5.   Thauer RK, Kaster A, Seedorf H, Buckel W (2008) Methanogenic Archaea:

605   Ecologically Relevant Differences in Energy Conservation. *Nature Rev Microbiol*

606   6:579–592.

607   6.   Conrad R (2007) Microbial Ecology of Methanogens and Methanotrophs.

608   *Advances in Agronomy* 96:1–63.

609   7.   Schaefer H, et al. (2016) A 21st-Century Shift from Fossil-Fuel to Biogenic

610   Methane Emissions Indicated by $^{13}CH_4$. *Science* 352(6281):80-84.

611   8.   Liu Y, Whitman WB (2008) Metabolic, Phylogenetic, and Ecological Diversity of

612 the Methanogenic Archaea. *Annals of the New York Academy of Sciences*

613 1125:171–189.

614 9. Borrel G, et al. (2019) Wide Diversity of Methane and Short-Chain Alkane

615 Metabolisms in Uncultured Archaea. *Nat Microbiol* 4:603-613.

616 10. Boyd JA, et al. (2019) Divergent Methyl-Coenzyme M Reductase Genes in a

617 Deep-Subseafloor Archaeoglobi. *ISME J* 13(5):1269–1279.

618 11. Evans PN, et al. (2019) An Evolving View of Methane Metabolism in the Archaea.

619 *Nat Rev Microbiol* 17(4):219–232.

620 12. Seitz KW, et al. (2019) New Asgard Archaea capable of Anaerobic Hydrocarbon

621 Cycling. *Nat Comm* 10:1822.

622 13. Laso-Pérez R, et al. (2016) Thermophilic Archaea Activate Butane via Alkyl-

623 Coenzyme M Formation. *Nature* 539(7629):396–401.

624 14. Chen SC, et al. (2019) Anaerobic Oxidation of Ethane by Archaea From a Marine

625 Hydrocarbon Seep. *Nature* 568(7750):108–111.

626 15. Wood TK (2017) Metabolic Manipulation of Methanogens for Methane

627 Machinations. *Microb Biotechnol* 10(1):9–10.

628 16. Goubeaud M, Schreiner G, Thauer RK (1997) Purified Methyl-Coenzyme-M

629 Reductase is Activated When the Enzyme-Bound Coenzyme F430 is Reduced to

630 the Nickel(I) Oxidation State by Titanium(III) Citrate. *Eur J Biochem* 243:110–

631 114.

632 17. Shima S, et al. (2012) Structure of a Methyl-Coenzyme M Reductase from Black

633 Sea Mats that Oxidize Methane Anaerobically. *Nature* 481(7379):98–101.

634 18. Ermler U, Grabarse W, Shima S, Goubeaud M, Thauer RK (1997) Crystal

635   Structure of Methyl-Coenzyme M Reductase : The Key Enzyme of Biological

636   Methane Formation. *Science* 278(5342):1457-1462.

637   19.   Grabarse W, Mahlert F, Shima S, Thauer RK, Ermler U (2000) Comparison of

638   Three Methyl-Coenzyme M Reductases from Phylogenetically Distant Organisms :

639   Unusual Amino Acid Modification , Conservation and Adaptation. *J Mol Biol*

640   303(2): 329-344.

641   20.   Zheng K, Ngo PD, Owens VL, Yang X, Mansoorabadi SO (2016) The

642   Biosynthetic Pathway of Coenzyme F430 in Methanogenic and Methanotrophic

643   Archaea. *Science* 354(6310):339– 342.

644   21.   Moore SJ, et al. (2017) Elucidation of the Biosynthesis of the Methane Catalyst

645   Coenzyme F430. *Nature* 543(7643):78–82.

646   22.   Grabarse W, et al. (2001) On the Mechanism of Biological Methane Formation:

647   Structural Evidence for Conformational Changes in Methyl-Coenzyme M

648   Reductase Upon Substrate Binding. *J Mol Biol* 309:315–330.

649   23.   Wongnate T, et al. (2016) The Radical Mechanism of Biological Methane

650   Synthesis by Methyl-Coenzyme M Reductase. *Science* 352(6288):953–958.

651   24.   Kahnt J, et al. (2007) Post-translational Modifications in the Active Site Region of

652   Methyl-Coenzyme M Reductase from Methanogenic and Methanotrophic Archaea.

653   *FEBS J* 274(18):4913–4921.

654   25.   Marlow JJ, et al. (2016) Proteomic Stable Isotope Probing Reveals Biosynthesis

655   Dynamics of Slow Growing Methane Based Microbial Communities. *Front*

656   *Microbiol* 7:1–21.

657   26.   Nayak DD, Mahanta N, Mitchell DA, Metcalf WW (2017) Post-translational

658   Thioamidation of Methyl-Coenzyme M Reductase, a Key Enzyme in

659   Methanogenic and Methanotrophic archaea. *Elife* 6(I):1–18.

660   27.   Deobald D, Adrian L, Schöne C, Rother M, Layer G (2018) Identification of a

661   Unique Radical SAM Methyltransferase Required for the sp3-C-Methylation of an

662   Arginine Residue of Methyl-coenzyme M Reductase. *Sci Rep* 8(1):1–12.

663   28.   Radle MI, Miller DV, Laremore TN, Booker SJ (2019) Methanogenesis Marker

664   Protein 10 (Mmp10) from *Methanosarcina acetivorans* is a Radical S -

665   Adenosylmethionine Methylase that Unexpectedly Requires Cobalamin . *J Biol*

666   *Chem* 10:jbc.RA119.007609.

667   29.   Mahanta N, Liu A, Dong S, Nair SK, Mitchell DA (2018) Enzymatic

668   Reconstitution of Ribosomal Peptide Backbone Thioamidation. *Proc Natl Acad Sci*

669   115(12):3030–3035.

670   30.   Wagner T, Kahnt J, Ermler U, Shima S (2016) Didehydroaspartate Modification in

671   Methyl-Coenzyme M Reductase Catalyzing Methane Formation. *Angew Chemie -*

672   *Int Ed* 55(36):10630–10633.

673   31.   Wagner T, Wegner C-E, Kahnt J, Ermler U, Shima S (2017) Phylogenetic and

674   Structural Comparisons of the Three Types of Methyl Coenzyme M Reductase

675   from *Methanococcales* and *Methanobacteriales*. *J Bacteriol* 199(16):e00197-17.

676   32.   Selmer T, et al. (2000) The Biosynthesis of Methylated Amino Acids in the Active

677   Site Region of Methyl-Coenzyme M Reductase. *J Biol Chem* 275(6):3755–3760.

678   33.   Nayak DD, Metcalf WW (2018) Genetic techniques for Studies of Methyl-

679   Coenzyme M Reductase from *Methanosarcina acetivorans* C2A. *Methods in*

680   *Enzymology* 613: 325-347.

681 34. Nayak DD, Metcalf WW (2017) Cas9-mediated Genome Editing in the

682   Methanogenic Archaeon *Methanosarcina acetivorans*. *Proc Natl Acad Sci U S A*

683   114(11):2976-2981.

684 35. Huynh K, Partch CL (2015) Analysis of Protein Stability and Ligand Interactions

685   by Thermal Shift Assay. *Curr Prot in Pro Sci* 79(1):1-14

686 36. Goenrich M, Duin EC, Mahlert F, Thauer RK (2005). Temperature Dependence of

687   Methyl-Coenzyme M Reductase Activity and of the Formation of the Methyl-

688   Coenzyme M Reductase Red2 State Induced by Coenzyme B. *J Biol Inorg Chem*

689   10:332-342.

690 37. Becker DF, Ragsdale SW (1998) Activation of Methyl-SCoM Reductase to High

691   Specific Activity After Treatment of Whole Cells with Sodium Sulfide.

692   *Biochemistry* 37(8):2639–2647.

693 38. Scheller S, Goenrich M, Boecher R, Thauer RK, Jaun B (2010) The Key Nickel

694   Enzyme of Methanogenesis Catalyses the Anaerobic Oxidation of Methane.

695   *Nature* 465(7298):606–608.

696 39. Edgar RC (2004) MUSCLE: Multiple Sequence Alignment with High Accuracy

697   and High tTroughput. *Nucleic Acids Res* 32(5):1792–1797.

698 40. Kearse M, et al. (2012) Geneious Basic: An Integrated and Extendable Desktop

699   Software Platform for the Organization and Analysis of Sequence Data.

700   *Bioinformatics* 28(12):1647–1649.

701 41. Kim SY, et al. (2012) Different Biosynthetic Pathways to Fosfomycin in

702   *Pseudomonas syringae* and *Streptomyces* Species. *Antimicrob Agents Chemother*

703   56(8):4175–4183.

704   42.   Metcalf WW, Zhang JK, Apolinario E, Sowers KR, Wolfe RS (2002) A Genetic

705   System for Archaea of the genus *Methanosarcina*: Liposome-mediated

706   Transformation and Construction of Shuttle Vectors. *Proc Natl Acad Sci*

707   94(6):2626–2631.

708   43.   Metcalf WW, Zhang JK, Wolfe RS (1998) An Anaerobic, Intrachamber Incubator

709   for Growth of *Methanosarcina* spp . on Methanol-Containing Solid Media. *Appl*

710   *Environ Microbiol* 64(2):768–770.

711   44.   Sowers KR, Boone JE, Gunsalus RP (1993) Disaggregation of *Methanosarcina*

712   spp. and Growth as Single Cells at Elevated Osmolarity. *Appl Environ Microbiol*

713   59(11):3832–3839.

714

715
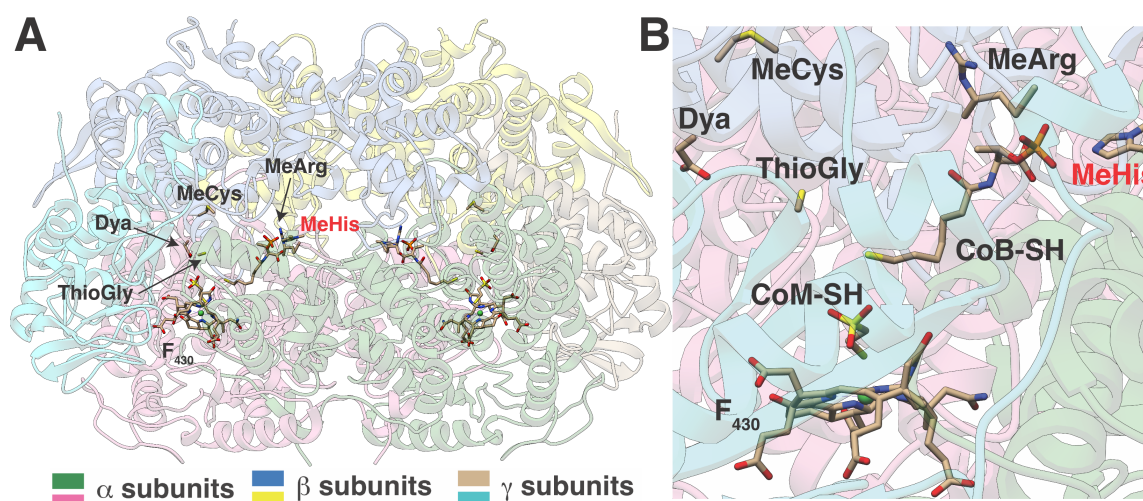
Figure 1: Crystal structure of MCR from *M. acetivorans*. A) The $\alpha_2\beta_2\gamma_2$ configuration of the MCR complex affinity-purified from *M. acetivorans* under aerobic conditions. The location of posttranslational modifications, the F430 cofactor, as well as coenzyme M (CoM-SH) and coenzyme B (coenzyme B-SH) are highlighted. No electron density corresponding to the affinity-tag was observed. **B)** A close-up of the active site within the McrA subunit in *M. acetivorans*. Dya: Didehydroasparate; MeCys: *S*-methylcysteine; MeArg: 5(S)-Methylarginine; MeHis: N^I-Methylhistidine; ThioGly: Thioglycine. The red shading of the MeHis label indicates that this residue is found within the other α-subunit, illustrating the fact that residues from both α-subunits are found in each active site.
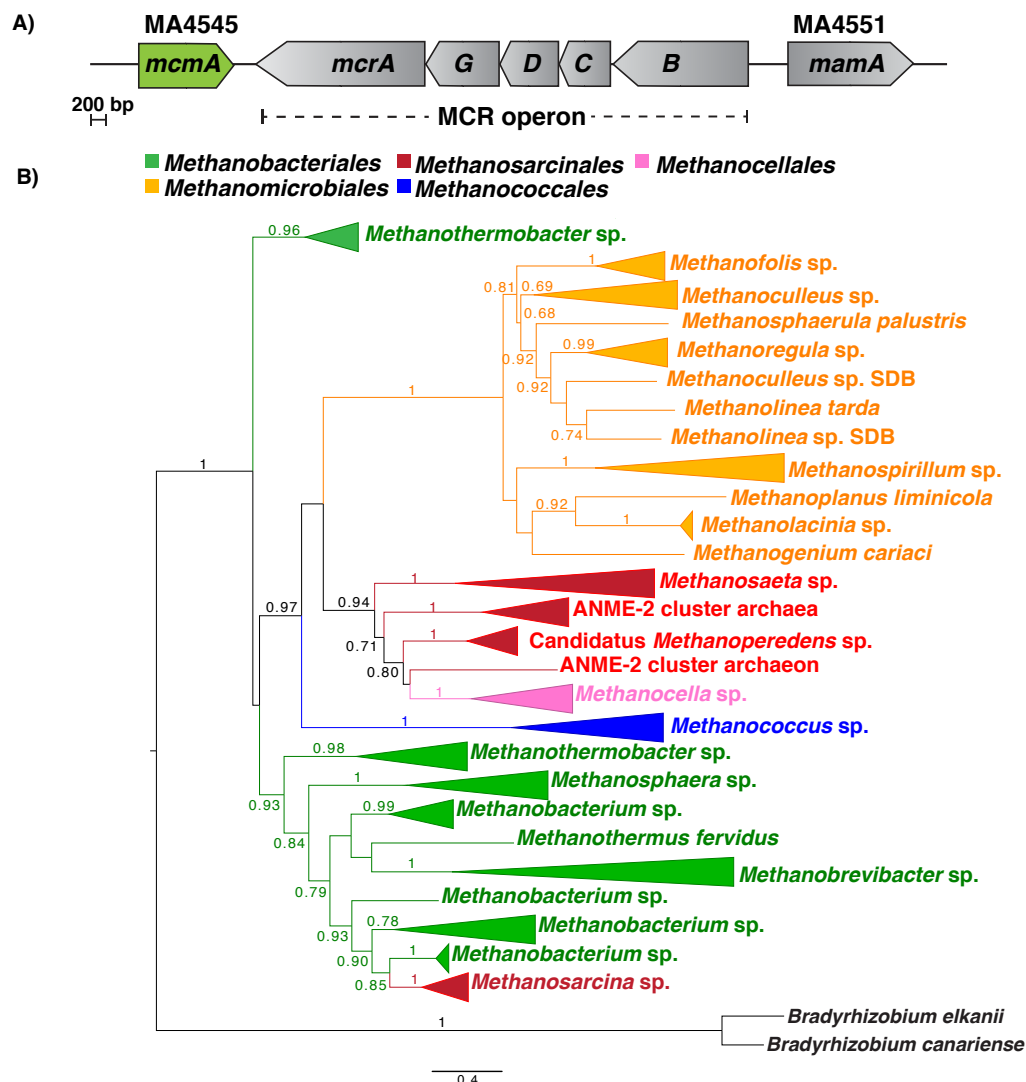
Figure 2: *In silico* analyses of McmA. A) Chromosomal organization of genes near the *mcr* operon in *Methanosarcina acetivorans.* Two *S*-adenosylmethionine (SAM) dependent methyltransferases are encoded on either side of the *mcr* operon. MA4551 encodes a radical SAM methyltransferase that was recently shown to be involved in the conversion of Arg285 in McrA to 5-(S)-methylarginine (27). We have named this gene *mamA* based on its proposed role (see text for details). **B)** A maximum-likelihood phylogenetic tree of the amino acid sequence of *mcmA* homologs in archaea. The node labels indicate support values calculated using the Shiomdaira-Hasegawa test using 1,000 resamples. Support values less than 0.6 have not been shown. The outgroup derives from bacterial McmA homologs (in black).
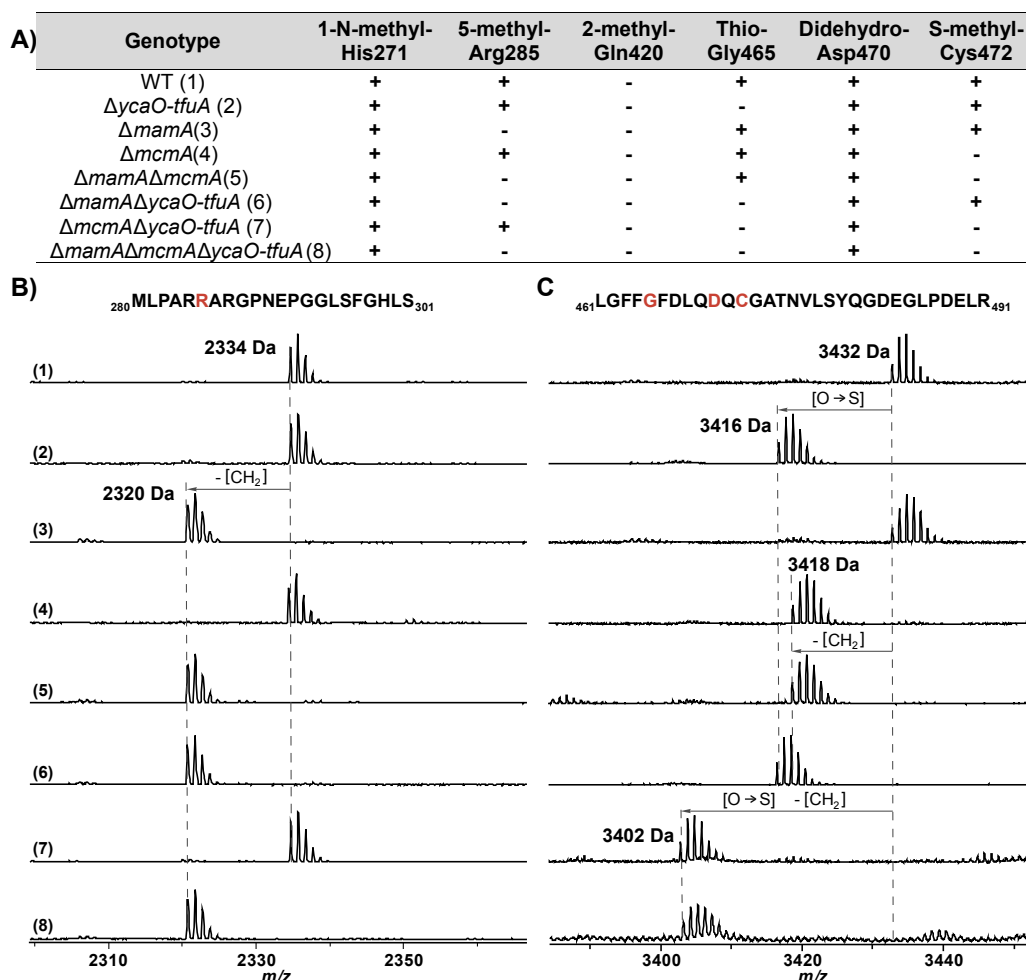
A)

Genotype	1-N-methyl-His271	5-methyl-Arg285	2-methyl-Gln420	Thio-Gly465	Didehydro-Asp470	S-methyl-Cys472
WT (1)	+	+	-	+	+	+
ΔycaO-tfuA (2)	+	+	-	-	+	+
ΔmamA (3)	+	-	-	+	+	+
ΔmcmA (4)	+	+	-	+	+	-
ΔmamAΔmcmA (5)	+	-	-	+	+	-
ΔmamAΔycaO-tfuA (6)	+	-	-	-	+	+
ΔmcmAΔycaO-tfuA (7)	+	+	-	-	+	-
ΔmamAΔmcmAΔycaO-tfuA (8)	+	-	-	-	+	-

Figure 3: MALDI-TOF MS analysis of McrA. **A)** A list of all the posttranslational modifications found in McrA derived from the various mutants as indicated. **B)** Spectrum of the indicated peptides, which were obtained after AspN and GluC digestion of MCR from wild-type (WWM60) and mutants lacking *ycaO-tfuA, mcmA,* and *mamA* in all possible combinations. The M_{280}-S_{301} peptide contains the Arg285 that is modified to 5-(S)-methylarginine by MamA. **C)** Spectrum of the indicated MCR tryptic peptide obtained from wild-type (WWM60) and mutants lacking *ycaO-tfuA, mcmA,* and *mamA* in all possible combinations. The L_{461}-R_{491} peptide contains the Gly465 and Cys472 that are modified to thioglycine and *S*-methylcysteine by *ycaO-tfuA* and *mcmA*, respectively, as well as the didehydroaspartate at Asp470. Modified residues are red in the peptide sequence.
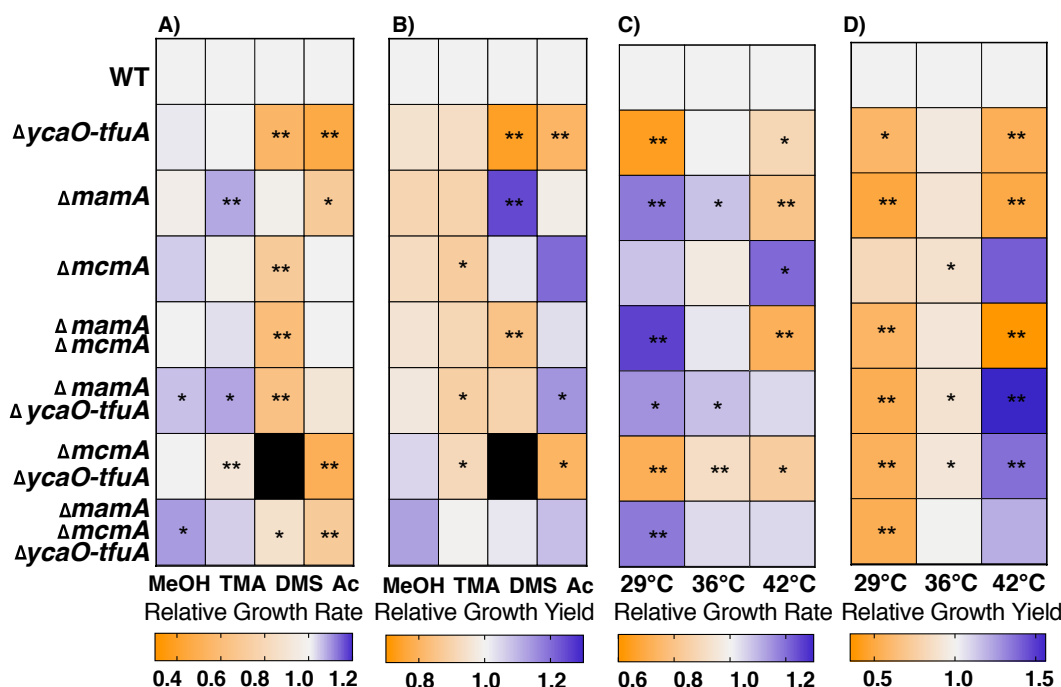
Figure 4: Phenotypic analyses on methanogenic substrates. Heat maps depicting **A)** growth rate or **B)** growth yield (measured as the maximum optical density at 600 nm) of mutants lacking *ycaO-tfuA, mcmA,* and *mamA* in all possible combinations relative to wild-type in bicarbonate-buffered High Salt medium supplemented with 125 mM methanol (MeOH), 50 mM trimethylamine hydrochloride (TMA), 20 mM Dimethylsulfide (DMS), or 40 mM sodium acetate (Ac) as the methanogenic substrates. All growth assays were performed at 36 °C. Heat maps depicting **C)** growth rate or **D)** growth yield (measured as the maximum optical density at 600 nm) of mutants in bicarbonate-buffered High Salt medium supplemented 50 mM TMA at three different temperatures as indicated. Statistically significant differences in growth parameters (p < 0.05 or p<0.01) relative to the wild-type as determined by a two-sided t-test are indicated with an * and ** respectively. The black box for the Δ*mcmA*Δ*ycaO-tfuA* mutant in DMS supplemented HS medium indicates that no measurable growth was detected after six months of incubation. The primary data used to construct the heatmaps is presented in Supplementary Tables 2-13.
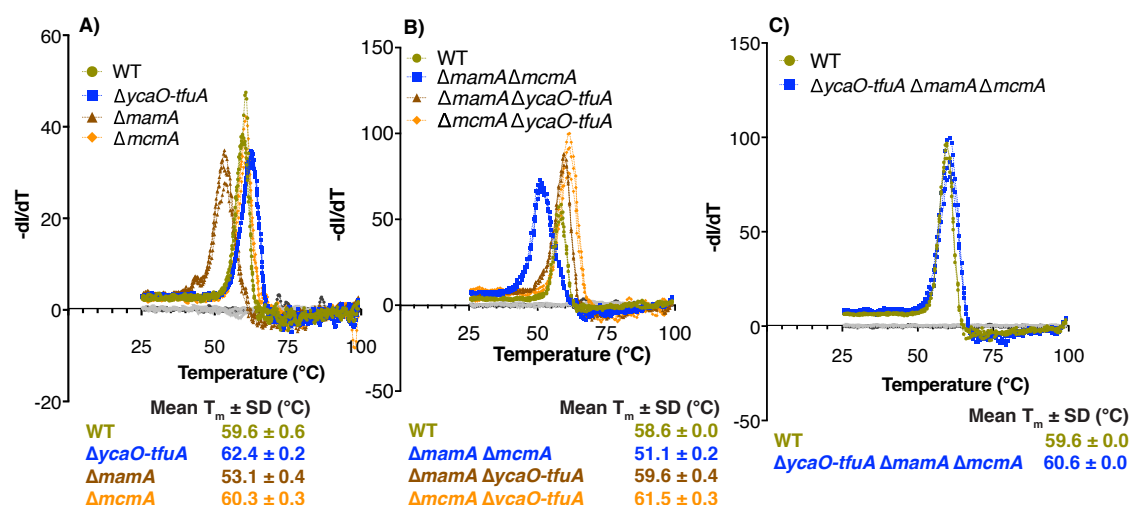
37

Figure 5: Melting temperature of the MCR complex. The thermal stability of the tandem-affinity tagged MCR complex purified from **A)** wild-type and single mutants lacking *ycaO-tfuA, mcmA,* or *mamA*, **B)** wild-type and double mutants lacking two of *ycaO-tfuA, mcmA,* and *mamA* in all possible combinations, and **C)** wild-type and the triple mutant lacking *ycaO-tfuA, mcmA,* and *mamA* was measured using the Sypro-Orange dye based thermofluor assay. The inflection point of the first differential curve for the fluorescence intensity relative to the temperature (-dI/dT) for each of three technical replicates was used to calculate the mean melting temperature (Tm) ± standard deviation (in °C) of the MCR complex. The no dye control (in grey) lacks the Sypro Orange dye and the no protein control (in black) was performed with elution buffer instead of purified protein.
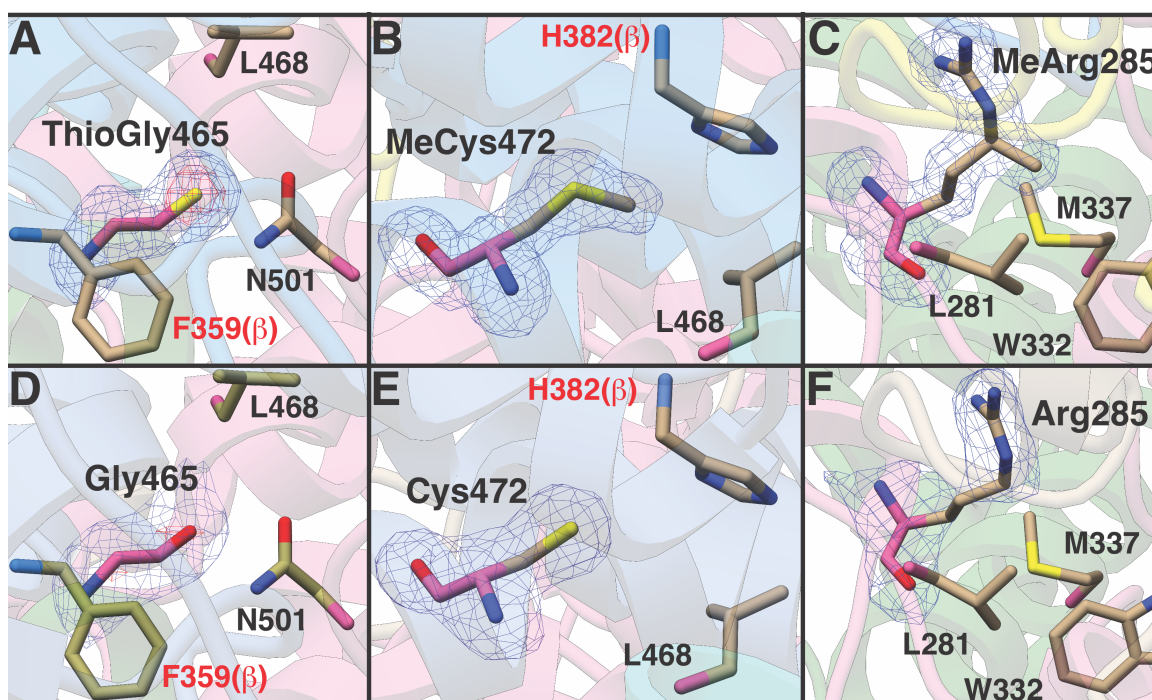
Figure 6: Absence of modified amino acids does not change the structure of MCR.
A), B), C) The local structure near Gly465 (modified to thioglycine), Cys472 (modified to *S*-methylcysteine), and Arg285 (modified to 5-(S)-methylarginine) in wild-type. **D), E), F)** The local structure near the unmodified Gly465 residue, unmodified Cys472 residue, and unmodified Arg285 residue in MCR derived from the Δ*ycaO-tfuA*, Δ*mcmA*, Δ*mamA* single mutants respectively. The structure of MCR purified from the double and triple mutants was indistinguishable from that show here, with RMSD between all pairs ranging between 0.1-0.3 Å.

39